

⁴⁷K. K. Seth, R. H. Tabony, E. G. Bilpuch, and H. W. Newson, Phys. Letters **13**, 70 (1964).

⁴⁸M. Divadeenam, private communication.

⁴⁹D. Slanina and H. McManus, Nucl. Phys. **A116**, 271 (1968).

⁵⁰M. P. Fricke, E. E. Gross, B. J. Morton, and A. Zucker, Phys. Rev. **156**, 1207 (1967).

⁵¹C. B. Fulmer, J. B. Ball, A. Scott, and M. L. Whiten, Phys. Letters **24B**, 505 (1967).

⁵²C. A. Engelbrecht and H. Fiedeldey, Ann. Phys. (N.Y.) **42**, 262 (1967).

⁵³P. A. Moldauer, Phys. Rev. **135**, B642 (1964).

⁵⁴C. E. Porter and R. G. Thomas, Phys. Rev. **104**, 483 (1956).

⁵⁵L. W. Weston, K. K. Seth, E. G. Bilpuch, and H. W. Newson, Ann. Phys. (N.Y.) **10**, 477 (1960).

⁵⁶J. H. Gibbons, R. L. Macklin, P. D. Miller, and J. H. Neiler, Phys. Rev. **122**, 182 (1961).

⁵⁷*Nuclear Data Sheets*, compiled by K. Way *et al.* (Printing and Publishing Office, National Academy of Sciences - National Research Council, Washington, D.C.).

⁵⁸S. A. Hjorth, Arkiv Fysik **33**, 183 (1966).

⁵⁹R. L. Kernell, Ph. D. thesis, University of Tennessee, 1968 (unpublished).

PHYSICAL REVIEW C

VOLUME 2, NUMBER 2

AUGUST 1970

Nuclear Level Structure of $^{169}\text{Er}^\dagger$

T. J. Mulligan and R. K. Sheline

Florida State University, Tallahassee, Florida 32306

and

M. E. Bunker and E. T. Jurney

University of California, Los Alamos Scientific Laboratory, Los Alamos, New Mexico 87544

(Received 24 February 1970)

Levels in ^{169}Er have been studied through the reactions $^{168}\text{Er}(d,p)^{169}\text{Er}$ and $^{170}\text{Er}(d,t)^{169}\text{Er}$, using 12-MeV deuterons, and via thermal-neutron capture in ^{168}Er . Over 40 states below 1.5 MeV are populated in the charged-particle reactions. These data, coupled with the ≈ 150 capture γ rays observed, lead to a level scheme that includes the following spectroscopic assignments (rotational band-head energy in keV, followed by the Nilsson single-particle state believed to be dominant): 0.0, $\frac{1}{2}^-$ [521], with associated rotational band to spin $\frac{11}{2}^-$; 92.2, $\frac{5}{2}^-$ [512], with band to $\frac{11}{2}^-$; 243.7, $\frac{7}{2}^+$ [633], with band to $\frac{13}{2}^+$; 562.1, $\frac{1}{2}^-$ [510], with band to $\frac{7}{2}^-$; 714.5, $\frac{3}{2}^-$ [521], with band to $\frac{11}{2}^-$; 823, $\frac{7}{2}^-$ [514], with band to $\frac{9}{2}^-$; 850, $\frac{5}{2}^-$ [523], with band to $\frac{11}{2}^-$; and 1081.8, $\frac{3}{2}^-$ [512], with band to $\frac{7}{2}^-$. In addition, a level at 860.2 keV is assigned as the head of a $K^\pi = \frac{3}{2}^+$ band that is mainly the $(K-2)$ γ -vibrational state associated with $\frac{7}{2}^+$ [633]. The data suggest that the 562.1-, 714.5-, and 1081.8-keV bands also have significant vibrational admixtures. Several features of the level scheme, including certain γ -ray branching ratios, are interpreted in terms of Coriolis mixing. The neutron separation energy for ^{169}Er is determined as 6003.1 ± 0.3 keV, and the Q value for the $^{170}\text{Er}(d,t)^{169}\text{Er}$ reaction is found to be -950 ± 30 keV.

I. INTRODUCTION

The nuclear energy level structure of ^{169}Er has been studied previously by several techniques. The work of Funke *et al.*¹ was concerned with the β decay of ^{169}Ho , which populates levels in ^{169}Er up to ≈ 0.95 MeV. The early (d,p) spectroscopic work of Isoya² was done with 80-keV resolution, using a target of natural Er. The (d,p) data of Harlan and Sheline³ were obtained using an enriched ^{169}Er target; however, the enrichment was only 77%, so that the observed spectrum was complicated by the presence of numerous peaks from impurity isotopes. Recently, Bonitz,⁴ from analysis of $(d,p\gamma)$ delayed-coincidence measurements, has established the existence of isomeric states at 92 and 244 keV.

In the present work, through analysis of high-resolution spectroscopic data from the reactions $^{168}\text{Er}(d,p)^{169}\text{Er}$, $^{170}\text{Er}(d,t)^{169}\text{Er}$, and $^{168}\text{Er}(n,\gamma)^{169}\text{Er}$, several new energy levels of ^{169}Er have been found, and an improved understanding of a number of the established levels below 1.4 MeV has been obtained. From analysis of the charged-particle relative cross sections, along with the level energies, it has been possible to group most of the observed low-energy states into rotational bands and to deduce the Nilsson single-particle character⁵ of these bands. In this analysis, the (n,γ) data have provided considerable guidance. For example, the observed primary (n,γ) transitions from the compound capture state (which has $I^\pi = \frac{1}{2}^+$) to low-lying states in the residual nucleus are almost always of dipole character, so that the *final* states can be as-

sumed to be of spin-parity $\frac{1}{2}^+$ or $\frac{3}{2}^+$. Also, from energy loops based on the low-energy (n, γ) data, one can deduce the γ -ray branching from individual states to lower states of known spin parity, which not only provides limitations on the spin parity of the initial state but often gives insight into its detailed character.

Following completion of the present experimental work, the unpublished (d, p) and (d, t) data of Tjøm and Elbek on ^{169}Er were made available to us. In most details, their data (now published⁶) confirm the present charged-particle results.

II. EXPERIMENTAL METHODS AND RESULTS

A. (d, t) and (d, p) Spectroscopy

The proton and triton spectra from the $^{168}\text{Er}(d, p)$, $^{169}\text{Er}(d, p)$ and $^{170}\text{Er}(d, t)$ reactions were obtained with a scaled-up Browne-Buechner-type single-gap broad-range magnetic spectrograph. The Florida State University Tandem Van de Graaff accelerator was used to generate the deuteron beam, which had an energy of 12 MeV and an intensity of 0.5–1.0 μA . A detailed account of the experimental arrangement is given in the work of Harlan and

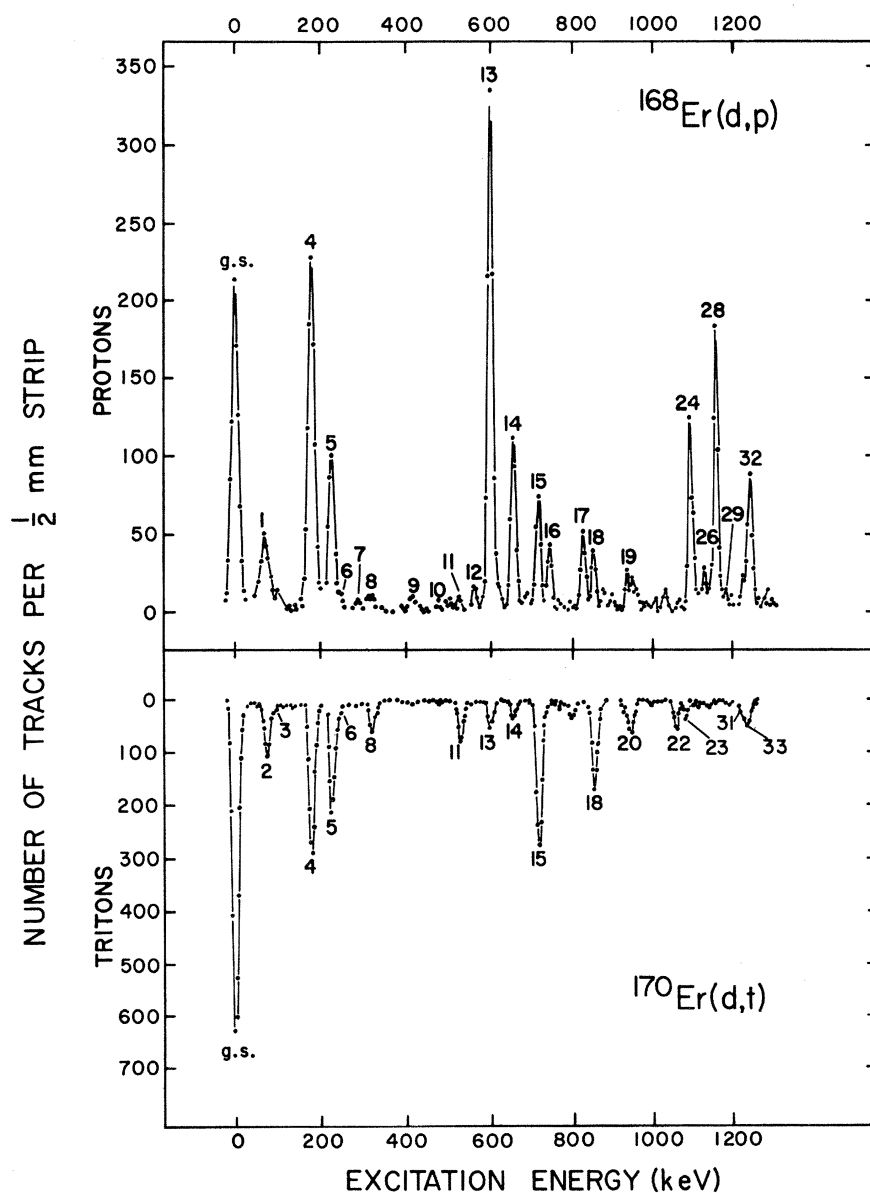


FIG. 1. Typical $^{168}\text{Er}(d, p)$ and $^{170}\text{Er}(d, t)$ data. The (d, p) data were taken at $\theta = 45^\circ$, and the (d, t) data were taken at $\theta = 75^\circ$. The peak numbers correspond to those given in Table II. Several of the weak, unlabeled peaks are due to impurities.

TABLE I. Spectrograph exposure conditions.

Reaction	Spectro- graph angle (deg)	Spectro- graph field (kG)	Exposure (μC)	Average resolution (FWHM) (keV)
$^{168}\text{Er}(d,p)^{169}\text{Er}$	25	9.5	10 000	22.5
$^{168}\text{Er}(d,p)^{169}\text{Er}$	45	8.6	10 000	15.0
$^{168}\text{Er}(d,p)^{169}\text{Er}$	60	8.6	6 620	16.5
$^{170}\text{Er}(d,t)^{169}\text{Er}$	60	12.5	15 000	16.6
$^{170}\text{Er}(d,t)^{169}\text{Er}$	75	12.5	15 000	15.0

TABLE II. Relative intensities of proton and triton groups from the reactions $^{168}\text{Er}(d,p)^{169}\text{Er}$ and $^{170}\text{Er}(d,t)^{169}\text{Er}$, and deduced level energies in ^{169}Er .

Peak symbol	E_{ex} (keV) (d,p)	Relative intensity					E_{ex} (keV) (d,t)
		(d,p) 25°	(d,p) 45°	(d,p) 60°	(d,t) 60°	(d,t) 75°	
g.s.	0.0	100	100	100	100	100	0.0
1	65 ± 2	13 ± 2	20 ± 3	7 ± 2	9 ± 2		65 ± 4
2	74 ± 3	8 ± 3	15 ± 2	19 ± 3	7 ± 2	16 ± 1	75 ± 3
3	93 ± 4	9 ± 2			1 ± 1	3 ± 1	95 ± 4
4	177 ± 2	52 ± 3	110 ± 7	128 ± 11	52 ± 4	47 ± 2	177 ± 3
5	224 ± 2	16 ± 1	45 ± 4	43 ± 5	37 ± 3	32 ± 2	225 ± 2
6	245 ± 2	4 ± 1	4 ± 1	4 ± 1	8 ± 1	4 ± 1	244 ± 2
7	285 ± 4		4 ± 1		1 ± 1	2 ± 1	285 ± 3
8	318 ± 3		5 ± 1	4 ± 1	13 ± 1	10 ± 8	320 ± 2
9	415 ± 3	16 ± 1	4 ± 1	3 ± 1		1 ± 1	416 ± 3
10	473 ± 5	3 ± 1	2 ± 1			1 ± 1	475 ± 4
11	528 ± 2		3 ± 1	8 ± 2	8 ± 1	11 ± 8	531 ± 3
12	557 ± 4	2 ± 1	5 ± 1		1 ± 1		558 ± 8
13	600 ± 2	79 ± 4	114 ± 8	83 ± 8	11 ± 1	9 ± 1	604 ± 2
14	654 ± 2	19 ± 2	40 ± 4	34 ± 4	5 ± 1	6 ± 1	659 ± 2
15	714 ± 3	37 ± 3	25 ± 3	23 ± 3	54 ± 4	41 ± 9	720 ± 2
16	740 ± 2	14 ± 1	15 ± 2	15 ± 3	8 ± 1	3 ± 1	741 ± 2
17	823 ± 3	9 ± 1	17 ± 2	19 ± 3	1 ± 1	1 ± 1	822 ± 2
18	849 ± 3	17 ± 2	13 ± 2	19 ± 3	30 ± 2	26 ± 1	856 ± 3
19	931 ± 4	5 ± 2	6 ± 1	15 ± 3		3 ± 1	927 ± 3
20					9 ± 2	10 ± 1	940 ± 2
21					1 ± 1	1 ± 1	990 ± 3
22					9 ± 1	7 ± 1	1052 ± 2
23					4 ± 1	5 ± 1	1077 ± 2
24	1083 ± 3	43 ± 2	33 ± 3	46 ± 5			
25					3 ± 1	2 ± 1	1095 ± 3
26	1118 ± 3		8 ± 1		1 ± 1	1 ± 1	1112 ± 4
27					2 ± 1	2 ± 1	1136 ± 3
28	1145 ± 3	36 ± 3	57 ± 5	77 ± 8			
29	1168 ± 2		3 ± 1	6 ± 1			
30						1 ± 1	1186 ± 4
31						3 ± 1	1218 ± 4
32	1232 ± 3	13 ± 3	27 ± 3	40 ± 5			
33					11 ± 2	8 ± 1	1234 ± 3
34						2 ± 1	1273 ± 3
35					9 ± 1	9 ± 1	1359 ± 3
36	1388 ± 2	118 ± 8	105 ± 10				
37					7 ± 1	7 ± 1	1394 ± 2
38	1415 ± 2	31 ± 3	31 ± 4		2 ± 1	2 ± 1	1413 ± 7
39	1459 ± 2	5 ± 1	8 ± 2				
40					9 ± 2	11 ± 1	1462 ± 2
41					34 ± 3	26 ± 1	1484 ± 2
42	1489 ± 2	216 ± 13	268 ± 20				
43					48 ± 3	39 ± 2	1529 ± 2

Sheline⁷. Targets for the (d,p) and (d,t) experiments were made with the Florida State University isotope separator by depositing ^{168}Er and ^{170}Er directly on thin carbon backings. Although the isotope-separated targets have the obvious advantage of extremely high isotopic purity (>99.9%), these targets are deposited in small spots (approximately of Tandem Van de Graaff beam size) of nonuniform density, making it virtually impossible to obtain accurate absolute cross sections. Details of the spectrograph exposures are summarized in Table I.

The charged particles were detected with an array of three 5-cm \times 25-cm Kodak NTA nuclear track plates. These plates were covered by an aluminum foil 0.12 mm thick in the (d,p) runs to stop deuterons. In the (d,t) runs, the plates were left uncovered. The proton (or triton) spectra recorded in the exposed plates were measured by counting the number of tracks in 0.5-mm strips with special scanning microscopes. Typical spectra are shown in Fig. 1. The spectra were analyzed by the use of a nonlinear least-squares code, which yielded positions and areas of individual peaks. These data were then converted to energies and relative cross sections through empirical energy and geometry calibrations of the spectrograph. The results are shown in Table II. The quoted energies represent weighted averages of the energies observed at the several angles. The energy errors were obtained by a systematic method which took into account the spread in the measured energies at the various angles, the effects of uncertainty in beam energy and spectrograph field, and the statistical accuracy of the Gaussian distributions fitted to the data.

A value of -950 ± 30 keV was obtained for the $^{170}\text{Er}(d,t)^{169}\text{Er}$ Q value. The rather large probable error is due mainly to the estimated uncertainty in the spectrograph magnetic field.

B. (n,γ) Spectroscopy

The thermal-neutron capture γ -ray data were taken at the internal target facility of the Los Alamos Omega West reactor. The external γ -ray beam was viewed through a collimating system by a ≈ 6 -cc Ge(Li) detector placed inside a divided annulus of NaI(Tl). The detector was operated in two modes: For γ -ray energies > 2 MeV, a coincidence was required between the pulse from the Ge(Li) detector and 511-keV pulses from each half of the NaI annulus. In this mode of operation, only the double-escape peaks are observed. For the low-energy portion of the spectrum ($E_\gamma < 2$ MeV), the annulus was operated as an anticoincidence shield

to reduce the background contribution from escaping Compton-scattered quanta. The energy resolution [full width at half maximum (FWHM)] of the detector ranged from ≈ 3 keV at 500 keV to ≈ 7 keV at 6 MeV. A more detailed description of this experimental arrangement can be found in the work of Journey, Motz, and Vegors.⁸

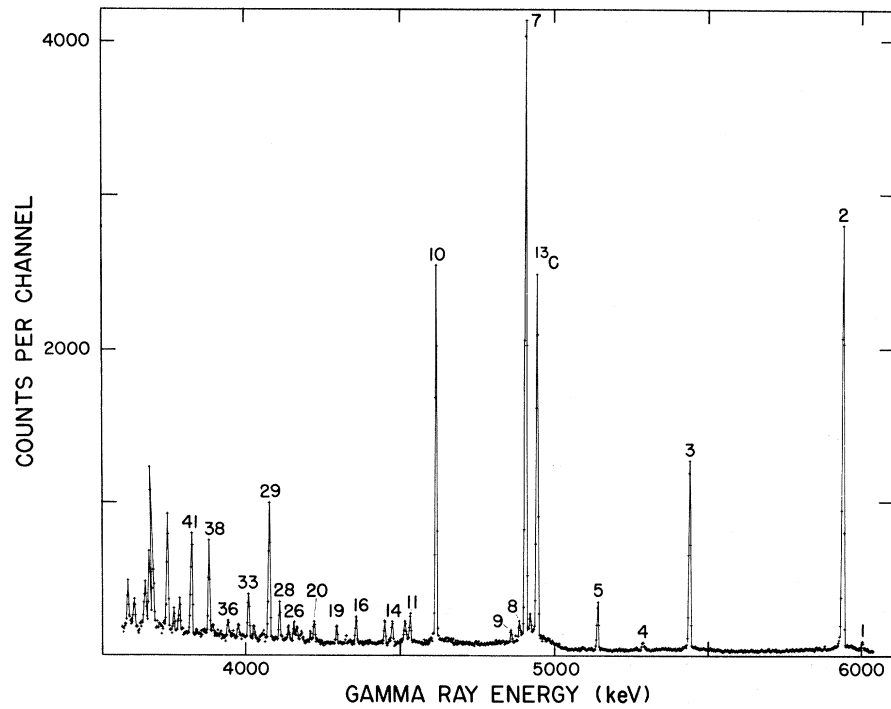
Additional measurements of the low-energy (10–130 keV) (n,γ) spectrum were made with a small Si(Li) detector placed in the external γ -ray beam. The energy resolution for this portion of the spectrum ranged from 0.45 keV FWHM at 25 keV to 0.75 keV at 100 keV.

The (n,γ) target, consisting of 0.498 g of Er_2O_3 enriched in ^{168}Er , had the following isotopic composition: ^{162}Er , $< 0.005\%$; ^{164}Er , $< 0.005\%$; ^{166}Er , $< 0.005\%$; ^{167}Er , 0.13%; ^{168}Er , 99.987%; ^{170}Er , $< 0.005\%$. Since the thermal (n,γ) cross section is 650 ± 30 b⁹ for ^{167}Er and 2.03 ± 0.41 b⁹ for ^{168}Er , approximately 4% of the neutron captures were in ^{167}Er . Through comparison of the gross (n,γ) spectrum with that obtained using a target of separated ^{167}Er , it was established that the following lines observed in the gross spectrum were due to $^{167}\text{Er}(n,\gamma)^{168}\text{Er}$: 79.8, 184.3, 198.2, 217.4, 284.6, and 815.9 keV. Since the energies of these lines are known quite accurately (79.80, 184.28, 198.24, 217.42, 284.65, and 815.95 keV, respectively) from the bent-crystal work of Koch,¹⁰ they were used as standards in constructing our energy calibration curves. It was also recognized that Koch's list¹⁰ of $^{167}\text{Er}(n,\gamma)$ transitions contains four transitions that are due solely to the $^{168}\text{Er}(n,\gamma)$ reaction: 64.545, 149.73, 151.61, and 159.59 keV. Of these, the 64.545- and 159.59-keV transitions were also used as energy calibration points. Additional points on the low-energy calibration curve were determined with a set of IAEA standard radioactive sources.¹¹ The IAEA sources also served as the primary standards in constructing detection efficiency curves for the Ge(Li) and Si(Li) detectors. The ^{169}Er γ -ray intensities were corrected for target self-absorption, the correction factor for this effect being ≈ 8 at 65 keV. Absolute intensities were determined relative to the thermal-neutron capture cross section of ^{197}Au .

At high energies (> 3.5 MeV), γ rays from $^{14}\text{N}(n,\gamma)^{15}\text{N}$ were used as standards¹² both of energy and of partial capture cross section. Reference 8 gives more detailed information concerning the calibration procedures.

A plot of the high-energy (n,γ) spectrum is given in Fig. 2. Figures 3 and 4 show parts of the low-energy (< 1.5 MeV) spectrum recorded with the Ge(Li) detector. Tables III and IV list the energies and intensities of all of the observed γ -ray transitions.

FIG. 2. High-energy $^{168}\text{Er}(n, \gamma)$ spectrum, obtained with a Ge(Li) spectrometer operated in the pair mode. Peak numbers correspond to those of Table III.



III. THEORETICAL CROSS-SECTION CALCULATIONS

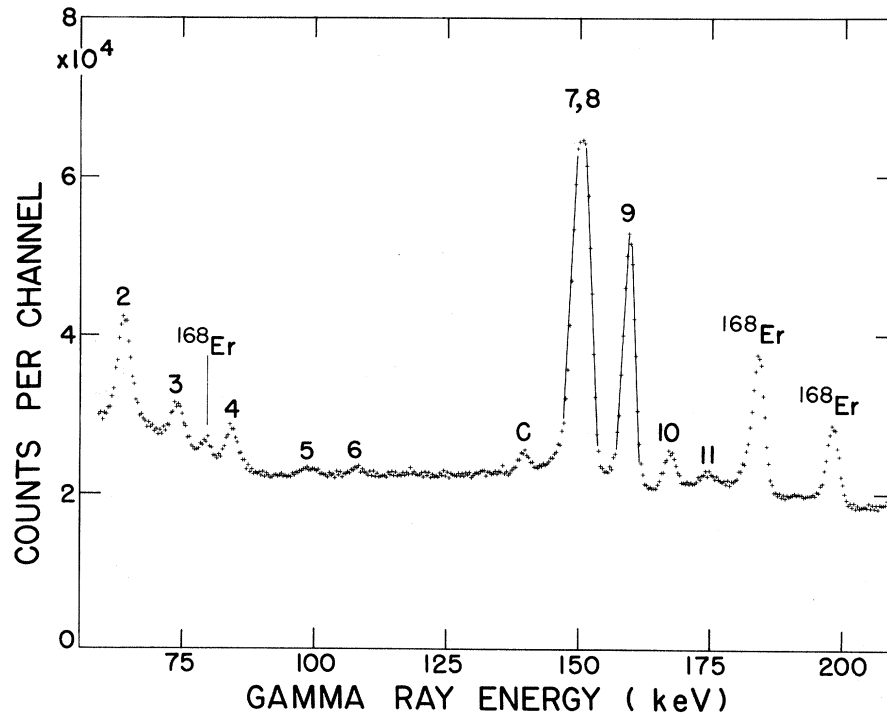
In the absence of state mixing, the theoretical cross sections for (d, p) and (d, t) reactions on deformed even-even target nuclei can be written as¹³⁻¹⁵

$$(d, p) \quad d\sigma/d\omega = 2C_{j,i}^2 U^2 \varphi_i(Q, \theta), \quad (1)$$

$$(d, t) \quad d\sigma/d\omega = \frac{20}{3} C_{j,i}^2 V^2 \psi_i(Q, \theta), \quad (2)$$

where $V^2 = 1 - U^2$ is the single-particle orbit occupation probability, the $\varphi_i(Q, \theta)$ [$\psi_i(Q, \theta)$] are distorted-wave Born-approximation (DWBA) predic-

FIG. 3. Low-energy $^{168}\text{Er}(n, \gamma)$ spectrum, obtained with a Ge(Li) spectrometer. Peak numbers correspond to those of Table IV. The peak C is due to an unassigned impurity.



tions of the intrinsic single-particle (d,p) [(d,t)] reaction cross sections, and the $C_{j,i}$'s are related to the Nilsson-model⁵ wave-function amplitudes $a_{i\Lambda}$. To calculate $\varphi_i(Q, \theta)$ and $\psi_i(Q, \theta)$, we have used the DWBA code JULIE.¹⁴ The values adopted for the optical-model parameters in the (d,p) calculation are those given by Rickey and Sheline,¹⁶ while the parameter values for the (d,t) calculation were taken from the work of Tjøm and Elbek.¹⁷ No lower cut-off radius was specified. Calculations were performed for $l=0-6$ and two different Q values, corresponding to excitation energies of 250 and 750 keV. The cross section at a given excitation energy was then determined from these values by interpolation (or extrapolation). Numerical values for V^2 were estimated from the following equation, taken from the work of Burke *et al.*,¹⁸ p. 47:

$$E = \Delta/2V(1 - V^2)^{1/2} - \Delta, \quad (3)$$

where E is the experimental quasiparticle energy and 2Δ is the so-called energy gap in even-even nuclei. The value assumed for Δ was 0.75 MeV. The predicted relative cross sections, normalized to a value of 100 for the $\frac{1}{2}, \frac{1}{2}^- [521]$ ground state,¹⁹ are displayed graphically in Fig. 5 [(d,p) , 45°] and Fig. 6 [(d,t) , 75°]. The possible effects of Coriolis mixing and vibrational admixtures on these cross sections are discussed in subsequent sections.

IV. INTERPRETATION OF THE EXPERIMENTAL RESULTS

The nuclear level scheme of ¹⁶⁹Er deduced from the present measurements is shown in Figs. 7 and 8. Most of the states included in the level scheme were directly seen in the (d,p) , (d,t) , or high-energy (n,γ) studies (see caption for Fig. 7). The existence of the other states is based on theoretical considerations and/or previous (β,γ) work.¹ In a number of cases, intensity and energy-balance arguments strongly suggest the assignment of specific low-energy γ rays as transitions between known levels. In this way, more precise values have been established for many of the level spacings.

The assignment of state configurations to the observed levels is based mainly on the following considerations: (1) the order of intrinsic states as predicted by the Nilsson model⁵ and the model of Soloviev, Vogel, and Junklaussen (SVJ)²⁰ (which includes pairing and quasiparticle-phonon interactions), (2) the characteristic energy-level spacing of rotational states, (3) comparison of the experimental (d,p) and (d,t) cross sections with the predictions of the Nilsson model, (4) spin-parity implications based on elementary γ -decay selection rules, (5) comparison of γ -ray branching ratios

with collective-model estimates (with correction for pairing and Coriolis-coupling effects), and (6) consistency with states observed in neighboring nuclei.

In analyzing the (d,p) and (d,t) data, we have assumed that an odd- A "vibrational" state is excited only through admixed single-particle components, i.e., that the collective vibrational component does

TABLE III. High-energy γ rays from the reaction ¹⁶³Er(n,γ)¹⁶⁹Er.

Line symbol	E_γ (keV)	E_{ex} (keV) ^a	I_γ ($\gamma/100n$) ^b
1	6002.4±0.7		0.12±0.03
2	5938.2±0.4	64.9±0.3	6.6 ±1.4
3	5441.0±0.4	562.1±0.3	3.0 ±0.6
4	5289.0±0.8	714.1±0.5	0.12±0.03
5	5142.9±0.7	860.2±0.4	0.76±0.16
6	4922.4±1.5	1080.7±1.2	0.27±0.11
7	4908.8±0.4	1094.3±0.3	10.3 ±2.1
8	4887.1±1.5	1116.0±1.2	0.31±0.13
9	4860.3±0.5	1142.8±0.4	0.18±0.04
10	4616.5±0.4	1386.6±0.3	6.0 ±1.2
11	4532.4±0.7	1470.7±0.4	0.44±0.10
12	4519.2±1.8	1483.9±1.5	0.14±0.10
13	4515.1±1.1	1488.0±0.8	0.30±0.10
14	4473.5±0.7	1529.6±0.4	0.34±0.08
15	4449.4±0.7	1553.7±0.4	0.36±0.13
16	4355.9±0.6	1647.2±0.3	0.42±0.09
17	4335.6±1.6	1667.5±1.3	0.05±0.02
18	4323.1±0.9	1680.0±0.6	0.11±0.03
19	4293.0±0.7	1710.1±0.4	0.27±0.06
20	4219.5±0.7	1783.6±0.4	0.39±0.09
21	4207.8±0.9	1795.3±0.6	0.18±0.05
22	4196.8±1.9	1806.3±1.6	0.05±0.02
23	4183.4±1.7	1819.7±1.4	0.09±0.03
24	4177.1±1.1	1826.0±0.8	0.19±0.06
25	4163.8±0.8	1839.3±0.5	0.29±0.07
26	4154.7±0.8	1848.4±0.5	0.31±0.08
27	4135.9±0.8	1867.2±0.5	0.27±0.07
28	4105.4±0.7	1897.7±0.4	0.61±0.13
29	4074.3±0.7	1928.8±0.4	2.3 ±0.5
30	4055.1±1.4	1948.0±1.1	0.14±0.05
31	4047.8±2.3	1955.3±2.0	0.09±0.05
32	4024.2±0.7	1978.9±0.4	0.22±0.05
33	4006.1±0.7	1997.0±0.4	0.82±0.17
34	3973.8±0.8	2029.3±0.5	0.24±0.06
35	3956.0±1.3	2047.1±1.0	0.10±0.04
36	3940.1±0.8	2063.0±0.5	0.33±0.08
37	3890.6±0.9	2112.5±0.6	0.18±0.05
38	3877.9±0.7	2125.2±0.4	1.5 ±0.3
39	3861.9±2.6	2131.2±2.3	0.07±0.03
40	3837.6±1.6	2165.5±1.3	0.05±0.02
41	3822.7±0.7	2180.4±0.4	1.7 ±0.4
42	3817.9±0.8	2185.2±0.5	0.41±0.12
43	3783.7±0.7	2219.4±0.4	0.55±0.14
44	3777.8±1.1	2225.3±0.8	0.17±0.06
45	3765.2±0.8	2237.9±0.5	0.36±0.10

^aBased on the deduced value $B_n=6003.1$ keV.

^bNumber of γ rays emitted per 100 neutron captures, based on a capture cross section of $\sigma_c=2.03$ b (Ref. 9).

TABLE IV. Low-energy γ rays from the reaction $^{168}\text{Er}(n, \gamma)^{169}\text{Er}$.

Line symbol	E_γ (keV)	I_γ ($\gamma/100n$) ^a	Line symbol	E_γ (keV)	I_γ ($\gamma/100n$) ^a
1	27.6 \pm 0.2	1.4 \pm 0.4	50	795.6 \pm 0.2	2.5 \pm 0.5
2	64.55 ^b	12.6 \pm 2.5	51	798.6 \pm 0.5	0.69 \pm 0.19
3	74.6 \pm 0.1	2.5 \pm 0.5	52	821.7 \pm 0.9 ^e	0.11 \pm 0.06
4	84.9 \pm 0.1	0.53 \pm 0.11	53	823.4 \pm 0.2 ^e	1.11 \pm 0.23
5	99.3 \pm 0.4 ^{c, d, e}	0.36 \pm 0.1	54	836.7 \pm 0.2 ^e	1.40 \pm 0.3
6	108.4 \pm 0.2	0.21 \pm 0.04	55	853.2 \pm 0.3 ^e	0.48 \pm 0.11
7	149.6 \pm 0.2	3.7 \pm 0.9	56	858.7 \pm 0.3 ^e	0.32 \pm 0.08
8	151.5 \pm 0.2	4.4 \pm 1.1	57	870.5 \pm 0.3 ^e	0.98 \pm 0.23
9	159.59 ^b	4.1 \pm 0.8	58	896.1 \pm 0.2 ^e	1.01 \pm 0.21
10	167.4 \pm 0.1	0.57 \pm 0.12	59	915.0 \pm 0.5 ^e	0.31 \pm 0.10
11	174.7 \pm 0.3 ^e	0.16 \pm 0.04	60	918.5 \pm 0.2 ^e	1.16 \pm 0.25
12	209.3 \pm 0.3 ^e	0.17 \pm 0.04	61	936.5 \pm 0.3 ^e	0.55 \pm 0.12
13	219.9 \pm 0.4 ^e	0.16 \pm 0.04	62	939.6 \pm 0.25	0.34 \pm 0.09
14	254.5 \pm 0.4 ^{c, e}	0.09 \pm 0.04	63	944.4 \pm 0.3	0.31 \pm 0.08
15	292.6 \pm 0.3 ^e	0.11 \pm 0.04	64	968.4 \pm 0.2	0.83 \pm 0.17
16	368.8 \pm 0.6 ^{c, e}	0.28 \pm 0.10	65	978.5 \pm 0.2 ^e	0.53 \pm 0.11
17	422.8 \pm 0.2 ^e	0.25 \pm 0.06	66	989.6 \pm 0.2	5.4 \pm 1.1
18	429.9 \pm 0.1	5.3 \pm 1.1	67	998.2 \pm 0.3 ^e	0.57 \pm 0.14
19	439.9 \pm 0.4 ^{c, e}	0.2 \pm 0.05	68	1002.1 \pm 0.2	1.00 \pm 0.23
20	470.2 \pm 0.4	2.4 \pm 0.6	69	1013.8 \pm 0.2 ^e	2.5 \pm 0.5
21	477.6 \pm 0.5 ^e	1.0 \pm 0.4	70	1019.9 \pm 0.2	1.8 \pm 0.4
22	497.5 \pm 0.1	8.6 \pm 1.7	71	1029.8 \pm 0.2	2.3 \pm 0.5
23	507.1 \pm 0.2	0.95 \pm 0.22	72	1042.5 \pm 0.3	0.89 \pm 0.19
24	524.8 \pm 0.1	2.8 \pm 0.6	73	1046.6 \pm 0.5 ^e	0.46 \pm 0.11
25	534.7 \pm 0.2	1.55 \pm 0.32	74	1052.6 \pm 0.2	1.97 \pm 0.40
26	545.0 \pm 0.6	0.27 \pm 0.08	75	1069.8 \pm 1.0 ^{c, e}	0.20 \pm 0.11
27	562.0 \pm 0.2	2.3 \pm 0.5	76	1078.5 \pm 0.3	0.93 \pm 0.21
28	579.3 \pm 0.4	0.17 \pm 0.04	77	1094.5 \pm 0.3	6.9 \pm 1.4
29	589.6 \pm 0.3	2.4 \pm 0.5	78	1117.8 \pm 0.4	0.63 \pm 0.13
30	599.2 \pm 0.2	3.9 \pm 0.8	79	1121.9 \pm 0.5 ^e	0.23 \pm 0.06
31	616.8 \pm 0.4	0.32 \pm 0.09	80	1270.1 \pm 1.1 ^e	0.13 \pm 0.07
32	622.8 \pm 0.6	0.15 \pm 0.06	81	1275.3 \pm 0.7 ^e	0.42 \pm 0.18
33	631.5 \pm 0.4 ^e	0.27 \pm 0.08	82	1277.6 \pm 1.0 ^e	0.25 \pm 0.15
34	640.0 \pm 0.2	0.84 \pm 0.18	83	1291.9 \pm 0.7 ^e	0.19 \pm 0.06
35	650.0 \pm 0.2	2.7 \pm 0.6	84	1295.5 \pm 0.5	0.31 \pm 0.08
36	663.0 \pm 0.6 ^e	0.64 \pm 0.23	85	1312.1 \pm 0.3	0.52 \pm 0.12
37	665.1 \pm 0.7	0.46 \pm 0.22	86	1315.4 \pm 0.6	0.23 \pm 0.07
38	682.4 \pm 0.2 ^e	1.19 \pm 0.25	87	1322.5 \pm 0.3	0.45 \pm 0.10
39	695.0 \pm 0.2	2.4 \pm 0.5	88	1330.8 \pm 0.4	0.30 \pm 0.08
40	704.9 \pm 0.2	2.0 \pm 0.4	89	1356.0 \pm 0.7	0.35 \pm 0.08
41	714.5 \pm 0.2	4.9 \pm 1.0	90	1359.6 \pm 0.5	0.47 \pm 0.11
42	732.2 \pm 0.2	4.3 \pm 0.9	91	1387.0 \pm 0.4	0.34 \pm 0.08
43	756.5 \pm 0.3 ^e	0.4 \pm 0.09	92	1393.3 \pm 0.6 ^e	0.28 \pm 0.08
44	760.7 \pm 0.2	0.54 \pm 0.11	93	1396.5 \pm 0.5 ^e	0.38 \pm 0.10
45	768.0 \pm 0.4 ^e	0.75 \pm 0.17	94	1407.9 \pm 0.4 ^e	0.42 \pm 0.10
46	772.1 \pm 0.3 ^e	1.43 \pm 0.03	95	1412.7 \pm 0.3 ^e	1.5 \pm 0.3
47	779.4 \pm 0.5 ^e	0.52 \pm 0.13	96	1417.8 \pm 0.6 ^e	0.3 \pm 0.9
48	785.4 \pm 0.2	3.5 \pm 0.8	97	1423.2 \pm 0.3 ^e	0.84 \pm 0.18
49	787.9 \pm 0.3	1.59 \pm 0.39			

^aNumber of γ rays emitted per 100 neutron captures, based on a capture cross section of $\sigma_c = 2.03$ b (Ref. 9). The quoted intensity errors include an assumed over-all uncertainty of $\pm 20\%$.

^bValue taken from Ref. 10; used as an energy standard.

^cQuestionable line; may not belong to ^{169}Er .

^dThis line is partly attributable to ^{168}Er γ rays of energy 98.98 and 99.29 keV (cf. Ref. 10).

^eNot included in the proposed decay scheme.

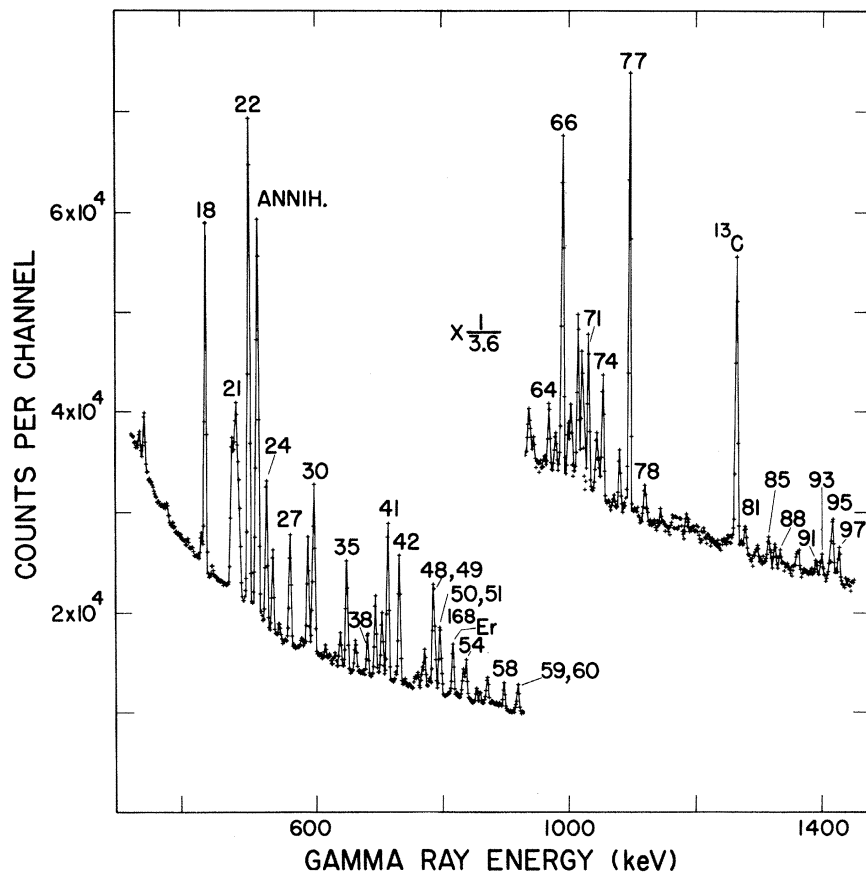


FIG. 4. Medium-energy $^{168}\text{Er}(n, \gamma)$ spectrum, obtained with a Ge(Li) spectrometer. Peak numbers correspond to those of Table IV.

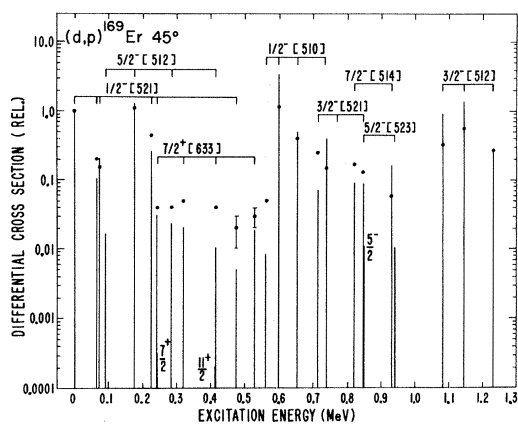


FIG. 5. Comparison of experimental and theoretical cross sections for the $^{169}\text{Er}(d, p)$ reaction at $\theta = 45^\circ$. Vertical bars indicate Nilsson-model estimates; dots correspond to experimental values. Both sets of values have been normalized so that the ground-state cross section equals 1.0 (in arbitrary units). For each rotational band, the vertical strikers (in sequence from left to right) indicate the positions of band members with spin values of $K, K+1, K+2$, etc. Where two states have nearly the same energy, one of the theoretical cross-section bars is labeled with the appropriate spin.

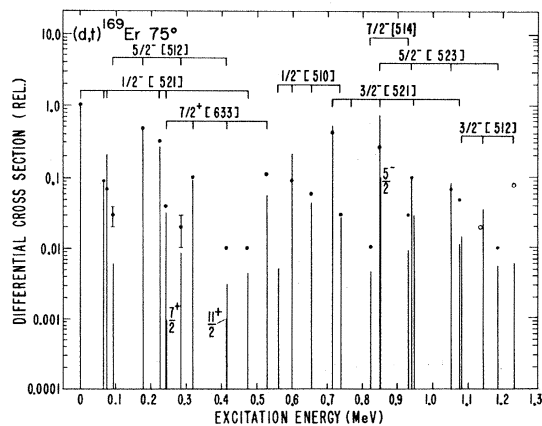


FIG. 6. Comparison of experimental and theoretical cross sections for the $^{170}\text{Er}(d, t)$ reaction at 75° . See caption of Fig. 5 for further description. Open circles represent questionable assignments.

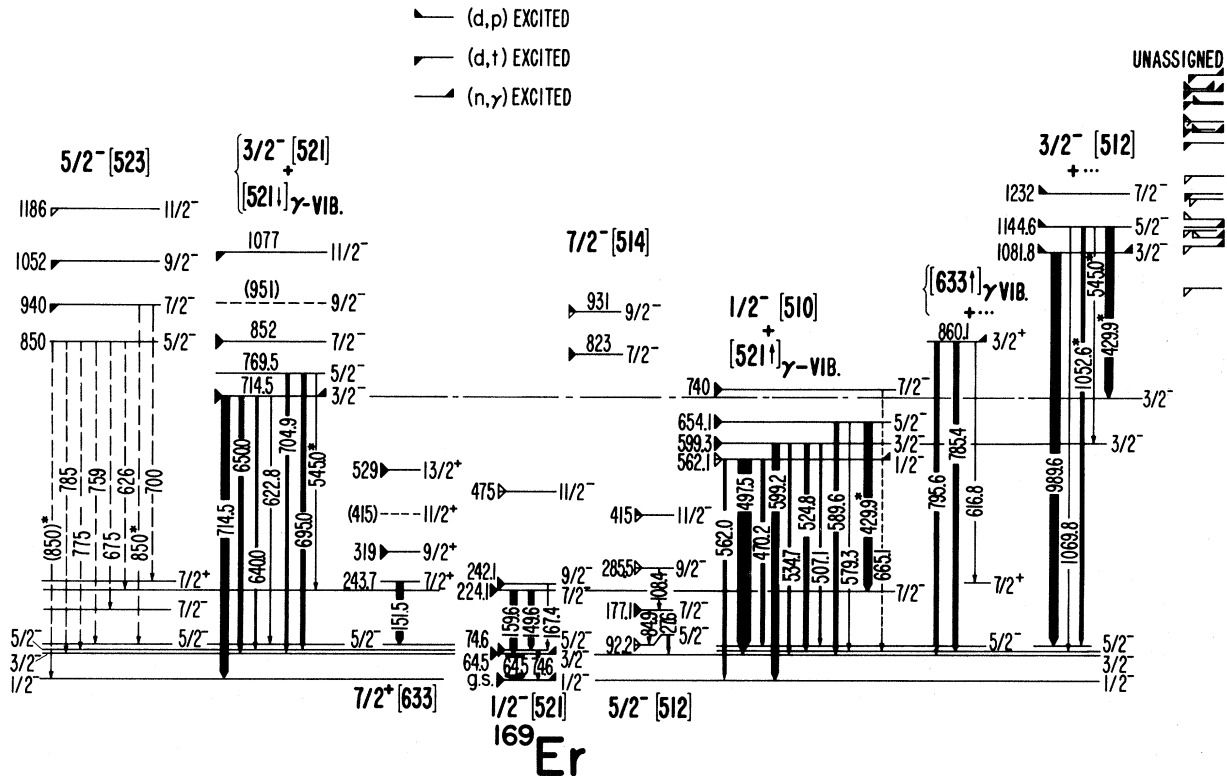


FIG. 7. Proposed level scheme of ^{169}Er . The flags at either end of the levels indicate population by the various reactions as defined at the top of the figure. The (n, γ) flags signify *direct* population from the compound state. Capture γ -ray transition intensities, uncorrected for internal conversion, are represented by the widths of the lines. Transitions used more than once in the scheme are marked with an asterisk. The dashed transitions at the left are a group of γ rays observed in the decay of ^{169}Ho (Ref. 1), some of which have been tentatively relocated in the decay scheme in order to achieve consistency with the present results (see text).

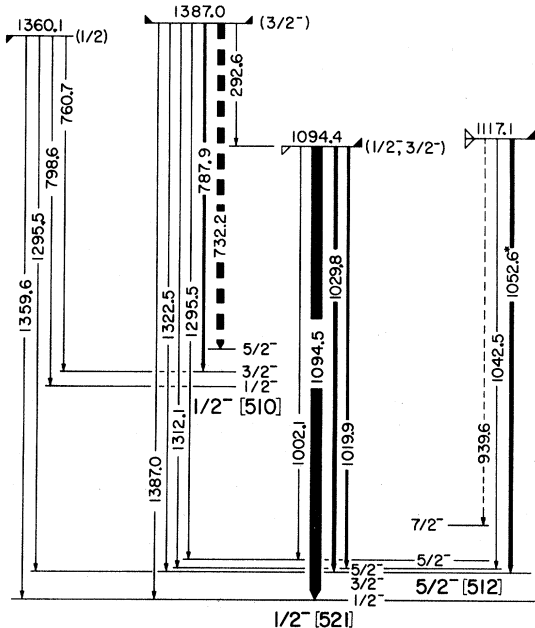


FIG. 8. Proposed γ decay of some well-established, but unassigned, high-energy states in ^{169}Er .

not contribute significantly to the observed cross section.

Through the use of the above guides, seven definite (and two probable) intrinsic states have been identified below 1.4-MeV excitation. Each of these states, along with its associated rotational band, is discussed separately below.

A. Ground-State Rotational Band

The ground-state spin of ^{169}Er is known²¹ to be $\frac{1}{2}$. The associated Nilsson orbital is clearly $\frac{1}{2}^- [521]$, an assignment strongly supported by all available data, as discussed below. Rotational states of this band up through the spin $\frac{7}{2}$ member were established in the prior work of Harlan and Sheline⁹ and Funke *et al.*¹

Since most levels of spin $\frac{1}{2}$ are populated observably by direct transitions in the (n, γ) reaction on an even-even target, one can reasonably expect to observe in the $^{169}\text{Er}(n,\gamma)$ spectrum a γ -ray transition corresponding to the binding energy of the last neutron in ^{169}Er . The highest-energy γ transition in the capture spectrum occurs at 6002.4 ± 0.7 keV. Since this energy fits well with the 5997 ± 12 keV

value for the neutron binding energy given by Harlan and Sheline,³ it is assumed that the weak 6002.4-keV transition proceeds to the ground state. However, from other energy sums involving direct transitions to states of well-established energy, we obtain a "best" value for the neutron binding energy of 6003.1 ± 0.3 keV. Thus, the next observed primary γ transition (5938.2 ± 0.4 keV) must proceed to a state of excitation energy 64.9 ± 0.3 keV, which is consistent with the established^{1,3} location of the $\frac{3}{2}^-$ member of the ground-state band. It is interesting to note that the intensity ratio of the primary (n, γ) transitions to the $\frac{3}{2}^-$ and $\frac{1}{2}^-$ members is 55:1. We assume that this very unequal branching is related to the complex nature of the compound capture state, dealt with by the Porter-Thomas²² theory.

In the present work, the observed charged-particle relative cross sections to the states of approximate energy 0, 65, 74, 224, 245, and 475 keV are consistent with the respective assignment of these states as the spin $\frac{1}{2}$, $\frac{3}{2}$, $\frac{5}{2}$, $\frac{7}{2}$, $\frac{9}{2}$, and $\frac{11}{2}$ members of the $\frac{1}{2}^-$ [521] band. From energy balance and intensity considerations, the (n, γ) transitions observed at 64.5, 74.6, 159.6, 149.6, and 167.4 keV are assigned as intraband transitions (see level scheme, Fig. 7), yielding energies for the first four rotational members of 64.5 ($\frac{3}{2}^-$), 74.6 ($\frac{5}{2}^-$), 224.1 ($\frac{7}{2}^-$), and 242.1 keV ($\frac{9}{2}^-$).

Using the first three members of this band in the rotational formula²³

$$E_I = E_0 + A[I(I+1) + a(-1)^{I+1/2}(I + \frac{1}{2})\delta_{\kappa, 1/2}] + BI^2(I+1)^2 + \dots, \quad (4)$$

where $A = \hbar^2/2\mathcal{J}$ and a is the so-called decoupling parameter, the following parameter values (assuming $B=0$) were obtained:

$$A = 11.77 \text{ keV}, \quad a = 0.83.$$

Using these parameter values, we predict $\frac{7}{2}^-$, $\frac{9}{2}^-$, and $\frac{11}{2}^-$ rotational levels at energies of 225.3, 243.3, and 480.2 keV, respectively, which agree reasonably well with those actually observed. An improved fit is obtained if a small negative B value is assumed ($B \approx -3.5$ eV), in which case $A = 11.78$ keV and $a = 0.82$. The value deduced for a is in good agreement with the Nilsson theoretical⁵ value of 0.88 for the $\frac{1}{2}^-$ [521] band, calculated using model-parameter values of $\delta = 0.3$, $\kappa = 0.05$, and $\mu = 0.45$.

B. $\frac{5}{2}^-$ [512] Band

The first excited *particle* state of ^{169}Er predicted by the Nilsson model is $\frac{5}{2}^-$ [512]. This band is

characterized in the (d, p) and (d, t) reactions by the fact that most of the cross section is associated with the $\frac{7}{2}^-$ member (cf. Figs. 5 and 6). The β -decay data of Funke *et al.*¹ indicate that the $\frac{5}{2}^-$ band head is at 91 keV, with the $\frac{7}{2}^-$ member at about 176 keV. The present (d, p) and (d, t) data yield energies of 93 and 177 keV for these two states. In addition, the weakly excited states at 285 and 415 keV are assigned as the $\frac{9}{2}^-$ and $\frac{11}{2}^-$ band members, respectively.

The 27.6-keV capture γ -ray transition, which is undoubtedly identifiable with the 26-keV γ reported by Funke *et al.*,¹ is assigned as the transition between the states $\frac{5}{2}, \frac{5}{2}^-$ [512] and $\frac{3}{2}, \frac{1}{2}^-$ [521]. The energy of the $\frac{5}{2}^-$ band head is thus established as 92.2 keV. Bonitz,⁴ in his ($d, p\gamma$) delayed-coincidence work, has shown that the half-life of this state is 285 ± 20 nsec.

The 84.9-keV (n, γ) transition is presumed to be the same as the 82-keV transition reported by Funke *et al.*,¹ which is known to connect the $\frac{7}{2}^-$ and $\frac{5}{2}^-$ members of the $\frac{5}{2}^-$ [512] band. On this basis, an energy of 177.1 keV is obtained for the $\frac{7}{2}^-$ state. Based on the energy spacing between the spin $\frac{5}{2}$ and $\frac{7}{2}$ states, the value of the moment-of-inertia parameter is found to be $A = 12.13$ keV (assuming $B=0$). Using this value, one calculates that the $\frac{9}{2}^-$ and $\frac{11}{2}^-$ members should lie at 286.3 and 419.7 keV, respectively. It seems highly probable that the observed 108.4-keV γ ray is identifiable with the 108-keV $\frac{9}{2}^- - \frac{7}{2}^-$ transition seen in the $^{169}\text{Er}(d, p\gamma)$ reaction.⁴ The implied energy value for the $\frac{9}{2}^-$ state is thus 285.5 keV. The deviation between the experimental energies (285.5 and 415 keV) and those calculated above (286.3 and 419.7 keV) indicates that this band has a small, negative B coefficient (≈ 5 eV).

C. $\frac{7}{2}^+$ [633] Band

The lowest-lying *hole* configuration in ^{169}Er is expected to be $\frac{7}{2}^+$ [633], and there is evidence from the ^{169}Ho decay data¹ that the $\frac{7}{2}^+$ base state of this band is at ≈ 241 keV. In the present experiment, comparison of the (d, p) and (d, t) cross sections for populating the levels at about 319 and 529 keV indicates that these two states are *hole* states. This observation, combined with energy and relative cross-section considerations, suggests the respective assignment of these states as the spin- $\frac{9}{2}$ and spin- $\frac{13}{2}$ members of the $\frac{7}{2}^+$ [633] band. We see no evidence for a state at 504 keV, assigned as $\frac{13}{2}^+$ by Harlan and Sheline.³ One would not expect the $\frac{7}{2}^+$ band head to be observably excited in the (d, p) and (d, t) experiments; not only is the theoretical cross section very small, but this level is essentially degenerate in energy with the state $\frac{9}{2}, \frac{1}{2}^-$ [521], which is expected to have a much

larger cross section (cf. Figs. 5 and 6).

We consider it probable that the (n, γ) transition of energy 151.5 keV is identifiable with the 150-keV γ seen by Funke *et al.*¹ and the 149.5-keV γ seen by Bonitz,⁴ and that this transition proceeds between the $\frac{7}{2}^+$ band head and the state $\frac{5}{2}, \frac{5}{2}^-$ [512]. On this basis, the band-head energy is 243.7 keV. The half-life of this state is known from Bonitz's work⁴ to be 200 ± 10 nsec. Using the experimental energies quoted above for the $\frac{7}{2}^+$ and $\frac{9}{2}^+$ levels, we calculate a moment-of-inertia parameter value of $A = 8.36$ keV, which yields a predicted energy of about 411 keV for the $\frac{11}{2}^+$ member and 520 keV for the $\frac{13}{2}^+$ member. Since the energy of the $\frac{13}{2}^+$ state is found to be 529 keV, this band would appear to have a positive B coefficient of ≈ 12 eV, which revises the predicted energy of the $\frac{11}{2}^+$ member to about 414 keV (cf. Eq. 4). The fact that the moment-of-inertia parameter is considerably smaller for this band than for the other bands of this nucleus is typical of the $\frac{7}{2}^+$ [633] band in neighboring nuclei, an effect attributable to the strong Coriolis coupling between the $\frac{7}{2}^+$ [633] configuration and the higher-lying $\frac{5}{2}^+$ [642] and $\frac{9}{2}^+$ [624] states.

D. $\frac{1}{2}^-$ [510] Band

The next intrinsic state observed above the $\frac{7}{2}^+$ [633] band head is a $K = \frac{1}{2}$ state, which appears to have the Nilsson configuration $\frac{1}{2}^-$ [510] as its dominant single-particle component. Harlan and Sheline³ previously identified the spin $\frac{3}{2}, \frac{5}{2},$ and $\frac{7}{2}$ band members through analysis of (d, p) spectra.

Results obtained on this band in the present work are as follows. A state at 562.1 ± 0.3 keV is populated by a direct high-energy γ -ray transition following thermal-neutron capture, which strongly suggests that the spin of this state is $\frac{1}{2}$ or $\frac{3}{2}$. The low-energy γ -ray spectrum includes transitions at $562.0 \pm 0.2, 497.5 \pm 0.1,$ and 470.2 ± 0.4 keV, which are energetically consistent with depopulation of the 562-keV level to the $\frac{1}{2}^-$ ground state, to the $\frac{3}{2}^-$ level at 64.5 keV, and to the $\frac{5}{2}^-$ [512] band head, respectively. The value deduced for the level energy is 562.1 ± 0.3 keV. The fact that no transition is observed to the 74.6-keV ($\frac{5}{2}^-$) level suggests that the state at 562 keV has spin $\frac{1}{2}$ rather than $\frac{3}{2}$. It is assumed that this state is the same as that observed at about 557 keV in the (d, p) and (d, t) spectra. From the relative (d, p) and (d, t) cross sections, it is evident that the 562.1-keV state is mainly a *particle* excitation rather than a *hole* excitation, as are also the states at about 600, 655, and 740 keV. The relative (d, p) cross sections to these four levels, on the assumption that they are of spin $\frac{1}{2}, \frac{3}{2}, \frac{5}{2},$ and $\frac{7}{2}$, respectively, are reasonably consistent with the Nilsson-model predictions for the orbital $\frac{1}{2}^-$ [510] (cf. Fig. 5).

The capture γ rays of energy 599.2, 534.7, 524.8, and 507.1 keV are energetically consistent with their placement as transitions from the $\frac{3}{2}^-$ band member (at 599.3 keV) to the $\frac{1}{2}^-, \frac{3}{2}^-,$ and $\frac{5}{2}^-$ members of the ground-state band and to the $\frac{5}{2}^-$ [512] band head, respectively. Similarly, the 589.6-, 579.3-, and 429.9-keV γ rays fit energetically as transitions from the $\frac{5}{2}^-$ band member (at 654.1 keV) to the $\frac{3}{2}^-, \frac{5}{2}^-,$ and $\frac{7}{2}^-$ members of the ground-state band. It is also possible that the 665.1-keV transition proceeds between the $\frac{7}{2}^-$ member and the state $\frac{5}{2}, \frac{1}{2}^-$ [521], which would yield an energy of 739.7 keV for the initial $\frac{7}{2}^-$ state.

The rotational parameter values deduced from the energies of the first three band members (assuming $B = 0$) are

$$A = 11.68 \text{ keV}, \quad a = +0.062.$$

Using these values, one calculates that the $\frac{7}{2}^-$ level should occur at about 740.9 keV. A three-parameter fit to the states up through the $\frac{7}{2}^-$ level (assumed at 739.7 keV) yields values of $A = 11.75$ keV, $a = +0.54,$ and $B = -8$ eV.

The Nilsson model predicts that the $\frac{1}{2}^-$ [510] configuration should lie at a much higher excitation energy than 562 keV in ^{169}Er . However, similar $K^\pi = \frac{1}{2}^-$ states with large $\frac{1}{2}^-$ [510] components have been found in neighboring nuclei at energies between 0.5 and 1.0 MeV (cf. Fig. 3 of Reich and Bunker²⁴). This appearance of $\frac{1}{2}^-$ [510] at anomalously low excitation energy has been explained theoretically²⁰ as a consequence of mixing between the $\frac{1}{2}^-$ [510] state and the $(K-2)$ γ vibration associated with $\frac{5}{2}^-$ [512]. Detailed particle-phonon mixing calculations have not yet been done for ^{169}Er . However, SVJ²⁰ have carried out such calculations for the neighboring nuclei ^{167}Er and ^{169}Yb . In these two cases, the state analogous to the mixed $K = \frac{1}{2}$ state under discussion has a calculated $\frac{1}{2}^-$ [510] content of 30 and 37%, respectively, the remainder of the state being largely the indicated $(K-2)$ vibration. In the ^{169}Er case, a crude experimental estimate of the amount of $\frac{1}{2}^-$ [510] in the 562-keV band is obtainable from a comparison of the charged-particle cross-section data with the theoretical predictions (see Fig. 5). These data are consistent with the 562-keV band being about one-third $\frac{1}{2}^-$ [510], which compares favorably with the estimates²⁰ for ^{167}Er and ^{169}Yb . The fact that the pure $E2$ transition from the 562-keV ($\frac{1}{2}^-$) state to the $\frac{5}{2}^-$ [512] band head competes observably with the $(M1 + E2)$ transitions to the $\frac{1}{2}^-$ [521] band is undoubtedly related to the $(\frac{5}{2}^-$ [512], 2^+) vibrational component in the $K = \frac{1}{2}$ band.

E. $\frac{3}{2}^-$ [521] Band

There is a primary (n, γ) transition to a level at 714.1 ± 0.5 keV, and the (d, p) and (d, t) data clearly indicate that the dominant single-particle component of this state is of *hole* character. The only reasonable Nilsson assignment would appear to be $\frac{3}{2}, \frac{3}{2}^-$ [521]. In support of this assignment, a level is observed at ≈ 852 keV in the charged-particle work which exhibits the expected behavior of the $\frac{7}{2}, \frac{3}{2}^-$ [521] state in that it has a very large (d, t) cross section. The ratio of cross sections for the spin- $\frac{3}{2}$ and spin- $\frac{7}{2}$ members deviates somewhat from the theoretical prediction for a pure $\frac{3}{2}^-$ [521] band, but this is explainable as a Coriolis mixing effect, as discussed below. The 714.5-, 650.0-, and 640.0-keV capture γ rays fit energetically as deexcitation transitions from the $\frac{3}{2}^-$ band head to the $\frac{1}{2}^-$, $\frac{3}{2}^-$, and $\frac{5}{2}^-$ members of the ground-state band. In support of these assignments, the relative intensities of the three transitions are consistent with the theoretical predictions²⁵ for an initial state having $I = K = \frac{3}{2}$, assuming pure dipole radiation. The value deduced for the band-head energy is 714.5 ± 0.2 keV. Energetically, the weak 622.8 ± 0.6 keV γ ray fits as the transition from the 714.5-keV state to the $\frac{5}{2}^-$ [512] band head.

The $\frac{5}{2}^-$ rotational state, which Tjøm and Elbek⁶ have identified with a weakly excited level at ≈ 768 keV, was not observed in our (d, p) and (d, t) spectra. However, the 704.9-, 695.0-, and 545.0-keV capture γ rays fit energetically as the transitions from the $\frac{5}{2}^-$ member (at 769.5 keV) to the $\frac{3}{2}^-$, $\frac{5}{2}^-$, and $\frac{7}{2}^-$ members of the ground-state band. The relative intensities of these transitions are consistent with the Alaga²⁵ rules, assuming $M1$ multipolarity. Thus, although there are two other levels that differ by ≈ 545 keV (see below), we suspect that most of the 545.0-keV intensity is due to the above $\frac{5}{2}^- \rightarrow \frac{7}{2}^-$ transition.

The energy difference of the $\frac{3}{2}^-$ and $\frac{5}{2}^-$ band members yields a moment-of-inertia parameter value of $A = 11.0$ keV. Based on the simple $AI(I+1)$ formula, the calculated energies of the $\frac{7}{2}$, $\frac{9}{2}$, and $\frac{11}{2}$ members are then about 847, 946, and 1067 keV (whereas our Coriolis band-mixing calculations, discussed in a later section, suggest values of 847, 951, and 1079 keV). Observation of the $\frac{7}{2}^-$ member at ≈ 852 keV has already been mentioned. The fact that this level lies very near the state $\frac{5}{2}, \frac{5}{2}^-$ [523] is discussed in the next section. The triton group observed in the (d, t) work at 940 keV is undoubtedly due, in part, to the $\frac{9}{2}^-$ band member, but the state $\frac{7}{2}, \frac{5}{2}^-$ [523] is believed to make the largest contribution to this peak (see next section). Tjøm and Elbek,⁶ in their (d, t) work, have

in fact resolved a weak peak at ≈ 947 keV, which they assign as $\frac{9}{2}, \frac{3}{2}^-$ [521]. Finally, it appears reasonable to assign the level observed at 1077 keV as the state $\frac{11}{2}, \frac{3}{2}^-$ [521].

The summed (d, t) cross section to this $\frac{3}{2}^-$ band is a little over half as large as that predicted for a pure $\frac{3}{2}^-$ [521] state. It is reasonable to attribute part of this reduction to admixture of the $(K-2)$ vibrational state associated with the $\frac{1}{2}^-$ [521] configuration, particularly in view of the fact that Soloviev's particle-phonon calculations²⁰ for the analogous $\frac{3}{2}^-$ state in ^{171}Yb (an isotone of ^{169}Er) yield a $(K-2)$ admixture of 62%. However, both our calculations (see below) and those of Kanestrøm and Tjøm²⁶ (which utilize the data of Ref. 6) indicate that the observed deviations from theory of the (d, t) cross sections for this band are largely attributable to Coriolis mixing, and on this basis it appears that the $(K-2)$ admixture is not more than $\approx 25\%$.

F. $\frac{5}{2}^-$ [523] Band

According to the work of Funke *et al.*,¹ a state of ^{169}Er at 850 keV is populated from ^{169}Ho ($\frac{7}{2}^-$ [523]) by an allowed-unhindered β transition ($\log ft = 4.7$), which, in conjunction with the observed γ -decay mode, strongly suggests a $\frac{5}{2}, \frac{5}{2}^-$ [523] assignment for the daughter state. Since this state should have a rather small theoretical (d, t) cross section and is nearly degenerate in energy with the state $\frac{7}{2}, \frac{3}{2}^-$ [521], it was not resolved in our charged-particle work. Also, this level appears to be very weakly excited in the (n, γ) reaction, since the reported³ pair of transitions to the $\frac{3}{2}^-$ and $\frac{5}{2}^-$ members of the ground-state band (differing in energy by 10.1 keV) was not observed.

The $\frac{7}{2}^-$ member of this band is reported by Funke *et al.*¹ to lie at 920 keV, the supporting evidence consisting of two observed γ rays (845 ± 3 and 700 ± 10 keV) that fit energetically as transitions to the $\frac{5}{2}^-$ and $\frac{7}{2}^-$ members of the ground-state band. We see no evidence for the proposed 920-keV level in the (d, t) spectra. Since a "pure" $\frac{7}{2}, \frac{5}{2}^-$ [523] single-particle state should have a (d, t) cross section of about one-third that of the $\frac{3}{2}^-$ state at 714 keV, we consider it very unlikely that the $\frac{7}{2}, \frac{5}{2}^-$ [523] state is at 920 keV. On the other hand, the hole state observed at 940 keV, which has a (d, t) cross section close to that expected for $\frac{7}{2}, \frac{5}{2}^-$ [523], is a reasonable candidate for this assignment.

Since one expects the state $\frac{7}{2}, \frac{5}{2}^-$ [523] to be observably populated by a direct β transition from ^{169}Ho , we have explored other interpretations of the data of Funke *et al.*¹ to see if agreement with the present experiments could be reached. We note that the energy difference of the 850- and 700-keV γ transitions of Ref. 1 is essentially the same

as that of the states $\frac{5}{2}, \frac{5}{2}^- [512]$ and $\frac{7}{2}, \frac{7}{2}^+ [633]$, making it possible that these two transitions depopulate a state at ≈ 943 keV, which could then be identified with our observed 940-keV state. In further support of this proposal, we note that in ^{169}Yb , which has a level structure very similar to that of ^{169}Er , the two strongest deexcitation γ rays from the state $\frac{7}{2}, \frac{5}{2}^- [523]$ proceed to members of the $\frac{5}{2}^- [512]$ and $\frac{7}{2}^+ [633]$ bands.^{26,27} It is possible, of course, that the 850-keV transition is a doublet, as we indicate in Fig. 7; in fact, the coincidence intensities reported by Funke *et al.*¹ suggest the assignment of roughly half of the 850-keV intensity to each of the two indicated transitions.

The above reinterpretation leaves the 845-keV γ ray of Funke *et al.*¹ unassigned. However, since the total decay energy of ^{169}Ho is about 2.1 MeV, it is quite possible that this unassigned γ ray depopulates a higher-lying (>1 MeV) level.

Note added in proof: A recent study of the $^{169}\text{Ho} \rightarrow ^{169}\text{Er}$ γ -ray spectrum with a Ge(Li) spectrometer by Haustein^{27a} has revealed that the $\frac{5}{2}^-$ and $\frac{7}{2}^-$ members of the $\frac{5}{2}^- [523]$ band are at 852.9 and 940.9 keV, respectively. The $\frac{5}{2}^-$, 852.9-keV level decays essentially as shown in Fig. 7. The 940.9-keV level decays to the $\frac{3}{2}^-$, $\frac{5}{2}^-$, and $\frac{7}{2}^-$ members (and possibly to the $\frac{9}{2}^-$ member) of the ground-state band; also, there appear to be transitions from this state to the two lowest members of the $\frac{7}{2}^+ [633]$ band. However, Haustein finds that a sizeable fraction of the "700-keV" line reported in Ref. 1 is due to the 695- and 705-keV γ rays that leave the 769.5-keV level (Fig. 7). No evidence is found for the 845-keV line of Ref. 1.

On the assumption that the $\frac{3}{2}^- [523]$ band head is at 850 keV and the $\frac{7}{2}^-$ member is at 940 keV, the moment-of-inertia parameter value is $A = 12.8$ keV. The calculated position of the $\frac{9}{2}^-$ member is then 1055 keV, and it is reasonable on the basis of both energy and cross section to associate the level observed at 1052 keV in the (d, t) work with this state. Finally, the state $\frac{11}{2}, \frac{5}{2}^- [523]$, expected at about 1189 keV, is tentatively associated with the level observed at 1186 keV in the (d, t) experiments. Tjømm and Elbek⁹ have also concluded that the states they observed at 940, 1052, and 1186 keV in the (d, t) reaction are the $\frac{7}{2}^-$, $\frac{9}{2}^-$, and $\frac{11}{2}^-$ members of this band.

The analogous $K^\pi = \frac{5}{2}^-$ band in ^{171}Yb is predicted²⁰ to have a sizable admixture (38%) of the $(K+2)$ γ vibration built on the $\frac{1}{2}^- [521]$ state. Within the uncertainties of the present analysis, it is possible that the ^{169}Er 850-keV band has a similar structure.

G. $\frac{3}{2}^- [512]$ Band

The states at 1083 ± 3 , 1145 ± 3 , and 1232 ± 3 keV,

all strongly excited in the (d, p) reaction, are interpreted, respectively, as the $\frac{3}{2}^-$, $\frac{5}{2}^-$, and $\frac{7}{2}^-$ members of a band that has $\frac{3}{2}^- [512]$ as its main single-particle component. This conclusion is based, first of all, on the fact that the energies are compatible with an $I(I+1)$ sequence (assuming $K = \frac{3}{2}$), the implied rotational parameter value of $A \approx 12.6$ keV being quite reasonable. Secondly, the relative (d, p) cross sections to the three levels in question are consistent with the above interpretation, as can be seen by reference to both Fig. 5 and the empirical results of Burke *et al.*¹⁸ on the $\frac{3}{2}^- [512]$ bands of ^{173}Yb , ^{175}Yb , and ^{177}Yb . Also, the $I = \frac{3}{2}$ assignment for the 1083-keV level is consistent with the fact that this level is populated by a direct high-energy (n, γ) transition. Tjømm and Elbek, in their ^{169}Er work,⁶ have reported an additional state at 1341 keV, which they tentatively assign as $\frac{9}{2}, \frac{3}{2}^- [512]$.

The theoretical calculations of SVJ²⁰ for ^{171}Yb indicate that a $\frac{3}{2}^-$ band with a large $\frac{3}{2}^- [512]$ component can reasonably be expected to occur in ^{169}Er at ≈ 1100 keV. Other components predicted²⁰ to play a significant role in the makeup of this state are the vibrational structures $(\frac{7}{2}^- [514], 2^+)$ and $(\frac{1}{2}^- [510], 2^+)$. The fact that the summed (d, p) cross section to the lowest three band members is roughly half the theoretical single-particle value is probably due largely to the presence of these vibrational components.

The strong 989.6-keV capture γ ray fits energetically as the transition from the $\frac{3}{2}^-$ band head to the 92.2-keV ($\frac{5}{2}^-$) state. This assignment yields a revised band-head energy of 1081.8 keV. Our Nilsson-model transition-probability calculations indicate that the $\frac{3}{2}^- [512]$ band head should decay more strongly (by a factor of ≈ 40) to the $\frac{5}{2}^- [512]$ band head than to any other of the available final states. This strengthens our placement of the 989.6-keV transition and provides additional support for the $\frac{3}{2}^- [512]$ assignment.

It is possible that the 1069.8-, 1052.6-, and 545.0-keV γ rays represent transitions from the $\frac{5}{2}^-$ band member to the 74.6-, 92.2-, and 599.3-keV levels, which would give an energy for the initial state of 1144.6 keV. However, there are alternative placements in the level scheme for the 545.0- and 1052.6-keV transitions. We also note that the energy difference of the 1144.6- and 714.5-keV levels is 430.1 keV, and it is therefore possible that part of the strong 429.9 ± 0.1 -keV line is due to the transition between these two levels.

H. Other Possible Bands

Based on the relative (d, p) and (d, t) cross sections, the 823- and 931-keV levels are *particle* states. The most likely interpretation of these two

levels is that they are, respectively, the $\frac{7}{2}^-$ and $\frac{9}{2}^-$ members of the $\frac{7}{2}^- [514]$ band, which is expected at about this excitation energy. From the 108-keV energy difference of the assumed $\frac{7}{2}^-$ and $\frac{9}{2}^-$ states, the moment-of-inertia parameter value is calculated to be $A = 12.0$ keV, which implies that the $\frac{11}{2}^-$ member should lie at about 1063 keV. Tjøm and Elbek⁶ have observed a state at 1051 keV which they tentatively assign as $\frac{11}{2}, \frac{7}{2}^- [514]$.

A level at 860.2 ± 0.4 keV is populated by a direct high-energy (n, γ) transition, and there are three capture γ rays (616.8, 785.4, and 795.6 keV) that fit energetically as transitions from this level to the $\frac{7}{2}^+ [633]$ band head and to the $\frac{3}{2}^-$ and $\frac{5}{2}^-$ members of the ground-state band, respectively. Assuming these transitions to be placed correctly, one obtains an energy for the parent level of 860.1 ± 0.2 keV. Selection-rule arguments indicate a $\frac{3}{2}^+$ spin-parity assignment for this level. Examination of the calculations of SVJ²⁰ (for the isotone ^{171}Yb) reveals that the only low-spin state of energy ≤ 1 MeV that has not already been accounted for in the above discussion is one with $K^\pi = \frac{3}{2}^+$. This state is predicted to be largely the $(K-2)$ γ vibration associated with $\frac{7}{2}^+ [633]$, with a significant admixture of the single-particle state $\frac{3}{2}^+ [651]$. This complex state should have very small (d, p) and (d, t) excitation cross sections (assuming no $\frac{3}{2}^+ [402]$ admixture), consistent with the fact that it is not seen in these reactions. Another argument favoring this assignment is that both the 860.1-keV level and the well-established^{27,28} $\frac{3}{2}^+$ complex vibrational state (at 720 keV) in ^{169}Yb are strongly populated in the (n, γ) reaction. However, these two states deexcite entirely differently, the one in ^{169}Yb exhibiting strong decay to the $\frac{7}{2}^+ [633]$ band head and no observable branching to the $\frac{1}{2}^- [521]$ band.^{27,28} One obvious way to reconcile the difference in the decay modes of these two levels is to postulate that the ^{169}Er state contains a much smaller $(K-2)$ vibrational component than that involved in the ^{169}Yb state.

It is noted that the proposed γ -ray branching of the 860.1-keV state to the ground-state band is in serious disagreement with the theoretical²⁵ prediction for the case $I_i = K_i = \frac{3}{2}$, $L = 1$. This is not considered to be an argument against the $\frac{3}{2}^+$ assignment, however, since it is well known that $E1$ transitions often disobey the Alaga²⁵ rules.

I. Unassigned States

There is a direct (n, γ) transition to a level at 1094.3 ± 0.3 keV. The strength of this transition indicates that the final state undoubtedly has spin-parity $\frac{1}{2}^-$ or $\frac{3}{2}^-$. Four strong γ rays (1094.5, 1029.8, 1019.9, and 1002.1 keV) are observed

which fit energetically as deexcitation transitions from this level to the four lowest states of ^{169}Er , yielding an energy of 1094.4 ± 0.2 keV for the initial state.

Direct (n, γ) population of a state at 1116.0 ± 1.2 keV is observed, and two relatively strong low-energy γ rays (1052.6 and 1042.5 keV) are tentatively assigned as depopulating this state, giving a level energy of 1117.1 keV. As noted above, part (or all) of the observed 1052.6-keV line may be due to a transition out of the 1144.6-keV state. We note also that the 939.6 ± 0.5 -keV γ ray can be placed as the transition from the 1117.1-keV level to the 177.1-keV state. It seems likely that the 1117-keV state is identifiable with the 1118-keV level excited in the (d, p) reaction.

One of the strongest high-energy (n, γ) transitions proceeds to a level at 1386.6 ± 0.2 keV. This level, which almost certainly has $I^\pi = \frac{1}{2}^-$ or $\frac{3}{2}^-$, is also strongly populated in the (d, p) reaction. The capture γ rays of energy 292.6, 787.9, 1295.5, 1312.1, 1322.5, and 1387.0 keV fit energetically as deexcitation transitions from this state, as shown in Fig. 8. The state energy implied by the various energy sums is 1387.0 ± 0.3 keV. It is possible that the strong 732.2-keV γ is the transition to the 654.1-keV level, even though the energy sum in this case (1386.3 ± 0.3 keV) lies slightly outside the above limits of error. The decay mode of the 1387.0-keV level strongly favors $I^\pi = \frac{3}{2}^-$, rather than $\frac{1}{2}^-$. The large (d, p) cross section for exciting the 1387-keV level suggests that this state may be analogous to the $\frac{3}{2}^-$ ($K = \frac{1}{2}$) state observed^{18,28} in ^{169}Yb at 1350 keV.

There are four γ rays (1359.6, 1295.5, 760.7, and 798.6 keV) that fit as deexcitation transitions from the 1359-keV level populated in the (d, t) reaction (see Fig. 8). The deduced level energy is 1360.1 ± 0.3 keV. Since these four γ rays terminate at levels with I^π of $\frac{1}{2}^-$ or $\frac{3}{2}^-$, it is probable that the 1360-keV state has $I = \frac{1}{2}$. A positive-parity assignment seems likely since all of the $I^\pi = \frac{1}{2}^-$ hole states expected at this approximate energy have exceedingly small theoretical (d, t) cross sections.

J. Further Theoretical Considerations

We have explored the possible effects of Coriolis band mixing^{29,30} on the charged-particle cross sections and on certain γ -ray transition probabilities. In the cross-section calculations, our general approach has been virtually the same as that recently described by Kanestrøm and Tjøm,²⁶ and the reader is referred to their article for additional discussion. The only states included in the Coriolis diagonalizations were the seven known negative-parity bands. It has been assumed that vibrational

admixtures simply “dilute” the single-particle strength. Thus, if P_i is the fractional purity assumed for i th *unperturbed* rotational band, the (d, p) cross section for a typical Coriolis-mixed state should correspond to

$$\frac{d\sigma}{d\omega} = 2 \sum_i (P_i^{1/2} C_{j_i}^i \alpha_i U_i)^2 \varphi_i(Q, \theta), \quad (5)$$

where the α_i are the amplitudes of the admixed states, and the other symbols are as defined in Sec. III. One difference between our Coriolis diagonalization and that of Ref. 26 is that we have ad-

justed the free parameters $A_{KK'}$ (the Coriolis matrix elements), \mathfrak{I}_K (moments of inertia), and a_K (decoupling parameters) to give an accurate energy fit to the observed levels. In order to meet this boundary condition, the only parameter value that needed to be adjusted significantly away from the value given by simple theory was the Coriolis matrix element between $\frac{5}{2}^-$ [523] and $\frac{7}{2}^-$ [514], which had to be set at about one half the theoretical value of $(UU' + VV')A_{KK'}$. The $\hbar^2/2\mathfrak{I}$ values assumed for the unperturbed states ranged from 10.5 to 13.5 keV.

TABLE V. Comparison of experimental and theoretical $^{168}\text{Er}(d, p)^{169}\text{Er}$ cross sections.

I	$K^\pi [Nn_z \Lambda]$	Energy (keV)		Relative $(d\sigma/d\omega)(d, p)$, 45°				Exper
		exp	calc ^{a,c}	Theory (case 1) ^a pure ^d	Theory (case 1) ^a mixed ^c	Theory (case 2) ^b pure ^d	Theory (case 2) ^b mixed ^c	
1/2	1/2 ⁻ [521]	0	0	100	100	100	100	100
3/2		64.5	64.5	9	16	26	35	20
5/2		74.6	74.4	21	30	21	30	15
7/2		224.1	223.8	27	30	24	28	45
9/2		242.1	242.5	2.9	3.3	2.5	3.1	4
11/2		475	474.8	0.5	0.3	0.3	0.3	2
5/2	5/2 ⁻ [512]	92.2	92.3	1.8	2.5	0.5	0.6	...
7/2		177.1	176.8	131	144	120	125	110
9/2		285.0	285.2	2.2	3.5	3.1	4.7	4
11/2		415	415.2	1.0	1.2	0.6	0.6	4
1/2	1/2 ⁻ [510]	562.1	562.3	8	4.7	2.0	1.4	5
3/2		599.3	599.0	332	122	343	123	114
5/2		654.1	654.3	61	20	64	23	40
7/2		740	740.1	41	10	31	8	15
9/2		...	838.8	1.6	0.4	1.5	0.5	...
11/2		...	973.4	0.3	0	0.1	0	...
7/2	7/2 ⁻ [514]	823	823.3	9	12	15	21	17
9/2		931	930.0	17	15	16	13	6
11/2		...	1055.2	0.6	0.4	0.4	0.3	...
3/2	3/2 ⁻ [521]	714.5	714.5	8	10	4.9	8	25
5/2		769.5	769.6	0	0.4	0	1.2	...
7/2		852	847.3	9	1.6	9	1.8	13
9/2		...	950.8	0.4	1.6	0.5	2.2	...
11/2		1077	1079.0	0.2	0.4	0.1	0.2	...
5/2	5/2 ⁻ [523]	850 ^e	850.2	1.2	0.5	1.0	0.2	...
7/2		940	938.9	1.1	0.5	2.1	0.5	...
9/2		1052	1052.3	0.9	0.3	0.8	0.6	...
11/2		...	1190.2	0.1	0	0.1	0	...
3/2	3/2 ⁻ [512]	1081.8	1081.8	76	39	107	54	33
5/2		1144.6	1143.5	144	67	140	63	57
7/2		1232	1231.1	27	10	21	8	27
9/2		...	1339.7	2.5	0.8	2.1	0.7	...
11/2		...	1478.4	0.2	0	0.1	0	...

^aUsing $\kappa=0.05$, $\mu=0.45$, $\delta=0.3$.

^bUsing $\kappa=0.0637$, $\mu=0.42$, $\delta=0.28$.

^cIncluding effects of pairing, vibrational admixtures, and Coriolis mixing (see text).

^dIncluding correction for pairing.

^eFrom Ref. 1.

Typical results of our (d, p) cross-section calculations are displayed in Table V. To show the effect of changes in the basic Nilsson-model parameters, we have given the results for two different sets of values: (1) $\kappa=0.05$, $\mu=0.45$, $\delta=0.30$; (2) $\kappa=0.0637$, $\mu=0.42$, $\delta=0.28$. The κ, μ values of case (1) are from Nilsson's original paper,⁵ and the values of case (2) are from Gustafsson *et al.*³¹ In both cases, we have assumed the following values for the single-particle purities of the unperturbed states: $\frac{1}{2}^- [510]$, 40%; $\frac{3}{2}^- [521]$, 80%; $\frac{3}{2}^- [512]$, 50%; and all others, 100%.

It can be seen that in several instances the mixing calculations improve the fit between theory and experiment, but the over-all improvement is not dramatic. Similar results were obtained by Kaneström and Tjømm.²⁶ One of the larger discrepancies that remains is the fact that the $\frac{3}{2}^- [521]$ band members are excited much more strongly in the (d, p) reaction than is predicted, whereas the calculated (d, t) cross sections for this band are in good agreement with experiment. It is also noteworthy that some of the calculated cross sections are more sensitive to the choice of Nilsson-model parameter values than they are to the amount of mixing.

Using the mixed Nilsson-model wave functions from the above-described Coriolis diagonalizations, we have calculated a number of γ -ray transition probabilities, some of which have already been mentioned. In these calculations, pairing was taken into account through multiplication of each nonrotational transition-probability amplitude by the factor $(UU' \pm VV')$, where the arithmetic sign is + for magnetic multipoles and - for electric multipoles. The same magnetic g factors were used for all orbitals: namely, $g_R=0.3$, $g_I=0$, and $(g_s)_{\text{eff}}=f(-3.825)$, where the value selected for f was 0.6. The effective charge of the odd neutron was assumed to be $e_{\text{eff}}=1.0e$. Rotational $E2$ transition probabilities were calculated from the relation

$$B(E2) = (1/5\pi) [\delta ZR^2(1+0.5\delta)]^2 \langle C_{if} \rangle^2, \quad (6)$$

where the factor C_{if} is a Clebsch-Gordan coefficient.

The decay of the 92.2-keV $\frac{5}{2}^-, \frac{5}{2}^- [512]$ state is of particular interest since the lifetime of this level is known⁴ ($T_{1/2}=285$ nsec). This state decays mainly to the 64.5-keV $\frac{3}{2}^-$ level. Since the 27.6-keV connecting transition is stronger than the ground-state $E2$ transition by a large factor $\geq (14)$, we assume that the 27.6-keV transition is predominantly $M1$. This $M1$ transition is K forbidden and can proceed only through admixtures, the most important of which are assumed to be introduced through Coriolis coupling. Similar comments apply to the 17.6-

keV transition to the 74.6-keV $\frac{5}{2}^-$ level, which Bonitz reports⁴ to have a γ -ray intensity of 0.17 relative to $I_\gamma(27.6 \text{ keV})$. Offhand, it is not surprising that the 27.6- and 17.6-keV transitions are stronger than the 92.2-keV $E2$ transition, since the $\frac{5}{2}^- [512] \rightarrow \frac{1}{2}^- [521]$ single-particle $E2$ matrix element is among the smallest encountered^{32, 33} in the rare-earth region.

Within the framework of our seven-band Coriolis calculations, the 27.6-keV transition intensity results primarily from admixture of $\frac{5}{2}^-, \frac{3}{2}^- [521]$ in the 92.2-keV state, whereas the ground-state $E2$ transition speed arises mainly from admixture of $\frac{5}{2}^-, \frac{1}{2}^- [521]$ in the initial state (i.e., the 92.2-keV transition is predominantly rotational in character). Using the Nilsson-model parameter values of case 1, given above, we obtain a γ -decay probability of $\lambda_\gamma(27.6 \text{ keV})=4 \times 10^5 \text{ sec}^{-1}$, which is about 6 times larger than the experimental value of $\approx 7 \times 10^4 \text{ sec}^{-1}$ (deduced from the present data, the data of Bonitz,⁴ and theoretical conversion coefficients³⁴). There is no way to tell whether this discrepancy results from overestimation of the amount of band mixing or whether the Nilsson theory gives too large a value for the dominant single-particle $M1$ matrix element. In any case, agreement to within a factor of 6 in such calculations is as good as can be expected, considering the many uncertainties involved.

The calculated decay probability of the 92.2-keV ($E2$) ground-state transition is indeed quite small. For example, using $\kappa=0.0637$, $\mu=0.42$, and otherwise reasonable parameter values, we obtain a decay constant that is somewhat smaller than the experimental upper limit of $\lambda_\gamma(92 \text{ keV}) < 5 \times 10^3 \text{ sec}^{-1}$. However, this decay probability is critically dependent on the parameter values used, such as the value of the Coriolis matrix element between $\frac{1}{2}^- [521]$ and $\frac{3}{2}^- [521]$ (which is small and quite sensitive to the values chosen for κ and μ). Thus, although one can qualitatively understand the slowness of this transition, it is questionable whether one should attach any special significance to the exact values used for the adjustable parameters.

As mentioned previously, the $\frac{7}{2}^+ [633]$ band head has a measured half-life of 200 nsec.⁴ For the γ -decay probability of the transition to the $\frac{5}{2}^- [512]$ band head, we calculate $\lambda_\gamma(151 \text{ keV})=2 \times 10^7 \text{ sec}^{-1}$ (using $\kappa=0.0637$, $\mu=0.42$, and $\delta=0.28$), which is a factor of ≈ 10 larger than the experimental⁴ value. This transition probability is insensitive to the amount of Coriolis mixing, but the pairing reduction factor is quite large (≈ 80). The analogous $E1$ transitions in neighboring nuclei are in general quite slow; e.g., in ^{173}Yb , the hindrance factor (with pairing included) for the $\frac{7}{2}^+ [633] \rightarrow \frac{5}{2}^-, \frac{5}{2}^- [512]$ transition turns out to be $F_N \approx 100$, using the same

(κ, μ, δ) values as in the above ^{169}Er calculation.

The γ branching of the complex $\frac{1}{2}^-([510] + \dots)$ band presents certain interpretive difficulties. This band deexcites primarily to members of the $\frac{1}{2}^-([521])$ band. As mentioned above, the character of the 562-keV band is thought to be about one-third $\frac{1}{2}^-([510])$. One expects that this single-particle component should largely determine the transition probabilities to the ground-state band and that the transitions in question should be predominantly $M1$. The simple Alaga rules²⁵ cannot be used to test whether the $M1$ branching ratios are anomalous in this case, since $L = K_i + K_f$; instead, the individual transition rates must be calculated from the appropriate Nilsson wave functions. In our studies of this branching, we have used the mixed state wave functions from various seven-band Coriolis diagonalizations. For the transitions leaving the 562.2-keV band head, we obtain a theoretical ratio $I_\gamma^{M1}(\frac{1}{2}^- \rightarrow \frac{3}{2}^-) : I_\gamma^{M1}(\frac{1}{2}^- \rightarrow \frac{1}{2}^-)$ of about 4:1 (nearly independent of the model parameter values used), which compares favorably with the experimental ratio of 3.7:1. However, the decay modes of the other band members disagree seriously with the theoretical estimates. For example, for the branching from the $\frac{3}{2}^-$ (599.3-keV) state, a typical calculation yielded $I_\gamma^{M1}(\frac{3}{2}^- \rightarrow 1/\gamma) : I_\gamma^{M1}(\frac{3}{2}^- \rightarrow \frac{3}{2}^-) : I_\gamma^{M1}(\frac{3}{2}^- \rightarrow \frac{5}{2}^-) = 1.0 : 1.8 : 0.001$, which is to be compared with the ratios $I_\gamma(599 \text{ keV}) : I_\gamma(535 \text{ keV}) : I_\gamma(525 \text{ keV}) = 1.0 : 0.40 : 0.72$. We have tried varying, by modest amounts, the Nilsson-model parameters and the Coriolis-coupling matrix elements in an attempt

to obtain better agreement between theory and experiment. However, we have not found any set of parameters which yields a significantly better fit to the data than that indicated above. It is possible, of course, that certain of the deexciting transitions have been placed incorrectly in the decay scheme or that intensity errors have been introduced as a result of failure to resolve multiplet peak structures. However, since the $\frac{3}{2}^-$ and $\frac{5}{2}^-$ band members both appear to exhibit anomalous branching, we believe that the source of the discrepancy is in the theory rather than in the experiment. It is possible, for example, that admixtures of states with energies >1.1 MeV, not introduced in our Coriolis calculations, have an important influence on the $M1$ transition probabilities in question.

ACKNOWLEDGMENTS

We wish to thank Dr. F. A. Rickey, Jr., and Dr. M. J. Bennett for their help with the DWBA calculations, and we are grateful to J. W. Starner for his assistance with the Coriolis calculations. We are indebted to Dr. P. O. Tjøm for valuable discussions and for transmittal of a description prior to publication of his work on ^{169}Er . The excellent cooperation of the staff of the Tandem Van de Graaff and the plate counters (under the direction of Mrs. Mary Jones) at Florida State University, the operating staff of the Los Alamos Omega West reactor, and K. E. Chellis, who made the spectrograph targets, is gratefully acknowledged.

†Work supported by the U. S. Atomic Energy Commission, the Nuclear Program of the State of Florida, and the U. S. Air Force Office of Scientific Research.

¹L. Funke, H. Graber, K.-H. Kaun, H. Sodan, and J. Frána, Nucl. Phys. **86**, 345 (1966); L. Funke, H. Graber, K.-H. Kaun, and H. Sodan, Ph.D. thesis, Deutsche Akademie der Wissenschaften zu Berlin, 1969 (unpublished).

²A. Isoya, Phys. Rev. **130**, 234 (1963).

³R. A. Harlan and R. K. Sheline, Phys. Rev. **168**, 1373 (1968).

⁴M. Bonitz, Ph.D. thesis, Deutsche Akademie der Wissenschaften zu Berlin, 1969 (unpublished).

⁵S. G. Nilsson, Kgl. Danske Videnskab. Selskab, Mat.-Fys. Medd. **29**, No. 16 (1955).

⁶P. O. Tjøm and B. Elbek, Kgl. Danske Videnskab. Selskab, Mat.-Fys. Medd. **37**, No. 7 (1969).

⁷R. A. Harlan and R. K. Sheline, Phys. Rev. **160**, 1005 (1967).

⁸E. T. Journey, H. T. Motz, and S. Vegors, Nucl. Phys. **A94**, 351 (1967).

⁹Brookhaven National Laboratory Report No. BNL-325, 1966 (unpublished), 2nd ed., Suppl. No. 2.

¹⁰H. R. Koch, Z. Physik **192**, 142 (1966).

¹¹Obtained from International Atomic Energy Agency, Vienna, Austria.

¹²J. B. Marion, Nucl. Data **A4**, 301 (1968).

¹³G. R. Satchler, Ann. Phys. (N.Y.) **3**, 275 (1958).

¹⁴R. H. Bassel, R. M. Drisko, and G. R. Satchler, Oak Ridge National Laboratory Report No. ORNL-3240 (unpublished).

¹⁵R. H. Bassel, Phys. Rev. **149**, 791 (1968).

¹⁶F. A. Rickey, Jr., and R. K. Sheline, Phys. Rev. **170**, 1157 (1968), table on p. 1160.

¹⁷P. O. Tjøm and B. Elbek, Kgl. Danske Videnskab. Selskab, Mat.-Fys. Medd. **36**, No. 8 (1967), Table 1.

¹⁸D. G. Burke, B. Zeidman, B. Elbek, B. Herskind, and M. Olsen, Kgl. Danske Videnskab. Selskab, Mat.-Fys. Medd. **35**, No. 2 (1966).

¹⁹The notation used here is $I, K^\pi [Nn_z \Lambda]$. The quantum number symbols are defined in Ref. 5.

²⁰V. G. Soloviev, P. Vogel, and G. Jungklausen, Izv. Akad. Nauk SSSR Ser. Fiz. **31**, 518 (1967) [transl.: Bull. Acad. Sci. USSR, Phys. Ser. **31**, 515 (1967)].

²¹A. Y. Cabezas, I. Lindgren, and R. Marrus, Phys. Rev. **122**, 1796 (1961).

²²C. E. Porter and R. G. Thomas, Phys. Rev. **104**, 483 (1956).

- ²³A. Bohr and B. R. Mottelson, *At. Energ. (USSR)* **14**, 41 (1963) [transl.: *Soviet J. At. Energy* **14**, 36 (1963)].
- ²⁴C. W. Reich and M. E. Bunker, in *Proceedings of the International Symposium on Nuclear Structure, Dubna, 1968* (International Atomic Energy Agency, Vienna, Austria, 1968), p. 119.
- ²⁵G. Alaga, K. Alder, A. Bohr, and B. R. Mottelson, *Kgl. Danske Videnskab. Selskab, Mat.-Fys. Medd.* **29**, No. 9 (1955).
- ²⁶I. Kanestrøm and P. O. Tjøm, *Nucl. Phys.* **A138**, 177 (1969).
- ²⁷E. B. Shera, M. E. Bunker, R. K. Sheline, and S. H. Vegors, Jr., *Phys. Rev.* **170**, 1108 (1968).
- ^{27a}P. E. Haustein, M.S. thesis, Iowa State University, 1970 (unpublished).
- ²⁸W. Michaelis, F. Weller, H. Schmidt, G. Markus,

- and U. Fanger, *Nucl. Phys.* **A119**, 609 (1968).
- ²⁹A. K. Kerman, *Kgl. Danske Videnskab. Selskab, Mat.-Fys. Medd.* **30**, No. 15 (1956).
- ³⁰R. T. Brockmeier, S. Wahlborn, E. J. Seppi, and F. Boehm, *Nucl. Phys.* **63**, 102 (1965).
- ³¹C. Gustafsson, I.-L. Lamm, B. Nilsson, and S. G. Nilsson, *Arkiv. Phys.* **36**, 613 (1967) [Proceedings of the Lysekil Symposium (1966)].
- ³²C. W. Reich and M. E. Bunker, *Izv. Akad. Nauk SSSR Ser. Fiz.* **31**, 42 (1967) [transl.: *Bull. Acad. Sci. USSR, Phys. Ser.* **31**, 46 (1967)].
- ³³C. J. Orth, M. E. Bunker, and J. W. Starnes, *Phys. Rev.* **132**, 355 (1963).
- ³⁴R. S. Hager and E. C. Seltzer, California Institute of Technology Report No. CALT-63-60, 1967 (unpublished).

PHYSICAL REVIEW C

VOLUME 2, NUMBER 2

AUGUST 1970

g Factor of the 50-keV $\frac{3}{2}^-$ State in ^{223}Ra and the Internal Magnetic Fields at Ra Nuclei in Ferromagnets*

M. Levanoni and F. C. Zawislak†

California Institute of Technology, Pasadena, California 91109

(Received 27 January 1970)

The γ - γ perturbed angular correlation of the 236–50-keV cascade in ^{223}Ra has been investigated, yielding $g(\frac{3}{2}^-, 50 \text{ keV}) = +0.28 \pm 0.04$. The magnetic hyperfine fields experienced by Ra nuclei embedded in Ni, Co, and Fe lattices were found to be -30 ± 10 , -80 ± 16 , and -105 ± 20 kOe, respectively.

The hyperfine magnetic fields at the sites of impurity atoms diffused in ferromagnetic hosts have been observed to exhibit a frequent change of sign as a function of the atomic number of the impurity. This behavior can be qualitatively understood from the electron configuration of the impurity. From systematics, the hyperfine magnetic fields on “5d” impurity atoms diffused in Fe lattice should have a behavior similar to the fields observed on “4d” elements in the same host. In particular, the field on Ba in Fe is small,¹ $H_{\text{int}}(\text{Ba Fe}) = 0 \pm 100$ kOe and since Ra is the “5d” counterpart of the “4d” Ba (both terminate their respective series), a similar result for Ra seems likely. In this paper we describe the results of measurements of the hyperfine magnetic fields acting on radium nuclei in Fe, Co, and Ni hosts. As a probe in this field measurement, the nuclear magnetic moment of the first $\frac{3}{2}^-$ state of ^{223}Ra was used. In a preceding experiment, this magnetic moment was determined.

The experiments have been performed with the perturbed-angular-correlation (PAC) method. The levels of ^{223}Ra are populated by α decay of ^{227}Th , which in turn is fed by β decay of the 22-yr ^{227}Ac .

From the partial level diagram of ^{223}Ra shown in Fig. 1, it is clear that the measurement of the $\frac{3}{2}^-$ state requires the use of Ge(Li) spectrometers. The apparatus is the same as that described in the work of Levanoni, Zawislak, and Cook,² but two 5-cm³ planar Ge(Li) detectors were used. Figure 2 shows the low-energy spectrum of ^{227}Ac and daughters, with the γ lines of interest (50 and 236 keV), which in our experiment could be well resolved.

The γ - γ sequence $\frac{3}{2}^+(236 \text{ keV})\frac{3}{2}^-(50 \text{ keV})\frac{1}{2}^+$ was investigated. Using a liquid source of carrier-free ^{227}Ac activity in a dilute solution of HNO_3 , the angular-correlation function for this cascade was determined, yielding, after solid-angle correction, coefficients $A_2 = -0.205 \pm 0.005$, and $A_4 = 0$. This result is in agreement with a previous measurement,³ and also in agreement with the theoretical coefficients $A_2 = -0.20$ and $A_4 = 0$ assuming that both transitions are pure electric dipoles in accordance with conversion-electron data. These results also indicate that time-dependent quadrupole interactions, which could attenuate the angular-correlation function during the relatively long lifetime of the intermediate state, are negligible.